JACS
JOURNAL OF THE AMERICAN CHEMICAL SOCIETY
Article
pubs.acs.org/JACS

Tough Stimuli-Responsive Supramolecular Hydrogels with Hydrogen-Bonding Network Junctions

Mingyu Guo,[†,‡,#] Louis M. Pitet,[†,§,#] Hans M. Wyss,[†,∥] Matthijn Vos,[⊥] Patricia Y. W. Dankers,[†,‡] and E. W. Meijer*[,†,‡,§]

[†]Institute for Complex Molecular Systems, [‡]Laboratory of Chemical Biology, [§]Department of Chemistry and Chemical Engineering, [∥]Department of Mechanical Engineering, Eindhoven University of Technology, P.O. Box 513, NL 5600 MB Eindhoven, The Netherlands

[⊥]FEI Company, Achtseweg Noord 5, 5600 KA Eindhoven, The Netherlands

Supporting Information

ABSTRACT: Hydrogels were prepared with physical cross-links comprising 2-ureido-4[1H]-pyrimidinone (UPy) hydrogen-bonding units within the backbone of segmented amphiphilic macromolecules having hydrophilic poly(ethylene glycol) (PEG). The bulk materials adopt nanoscopic physical cross-links composed of UPy−UPy dimers embedded in segregated hydrophobic domains dispersed within the PEG matrix as comfirmed by cryo-electron microscopy. The amphiphilic network was swollen with high weight fractions of water ($w_{H_2O} \approx 0.8$) owing to the high PEG weight fraction within the pristine polymers ($w_{PEG} \approx 0.9$). Two different PEG chain lengths were investigated and illustrate the corresponding consequences of cross-link density on mechanical properties. The resulting hydrogels exhibited high strength and resilience upon deformation, consistent with a microphase separated network, in which the UPy−UPy interactions were adequately shielded within hydrophobic nanoscale pockets that maintain the network despite extensive water content. The cumulative result is a series of tough hydrogels with tunable mechanical properties and tractable synthetic preparation and processing. Furthermore, the melting transition of PEG in the dry polymer was shown to be an effective stimulus for shape memory behavior.

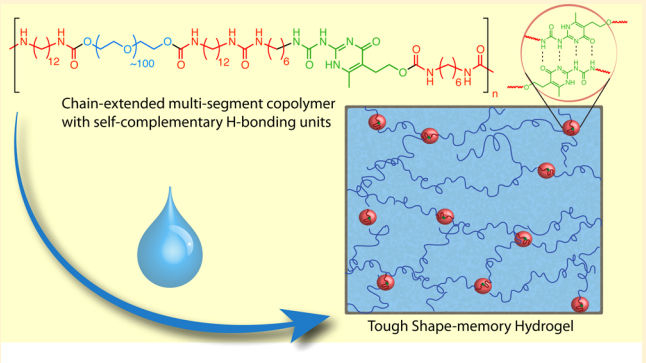

INTRODUCTION

Inspired by nature, there is dramatically increasing demand for synthetic biocompatible hydrogels that exhibit complex behavior, but are nonetheless conceptually easy to prepare and to process, while having accessible handles with which mechanical and physiological properties can be tailored.[1−10] Most synthetic hydrogels are brittle and therefore poor candidates for mimicking biomaterials such as cartilage. In addition to dramatic improvements in tensile toughness (i.e., work of extension W_e), molecular design can be used to impart hydrogels with a suite of attractive properties: high water uptake without sacrificing strength and resilience;[11,12] dynamic physical (e.g., noncovalent) cross-linkers to promote processability and self-healing;[13−16] and stimuli responsiveness, e.g., for shape memory behavior.[17−20] Recent examples illustrate astounding improvements in toughness and extensibility from intricate molecular makeup with finely tuned association characteristics.[21] However, designing soft materials with high toughness is still a challenge, as energy dissipation mechanisms are complex.[22,23]

Poly(ethylene glycol) (PEG) is an attractive candidate for biomedical applications. Features including hydrophilicity and a bulk melting temperature (T_m) of 40−50 °C are conducive to both hydrogelation and shape memory behavior near physiologically relevant conditions.[16,24−30] Often, processable hydrogel materials employ self-assembling block copolymers with segregated hydrophilic (e.g., PEG) and hydrophobic domains.[31−33] The cross-link density and composition can be systematically varied in an effort to tune the ultimate modulus and failure elongations, which cumulatively reflect the tensile toughness of the material.[34] It has been proposed that one of the critical features of the optimal molecular structure to form tough hydrogels include a strong, yet reversible interaction within segregated nanoscopic domains.[35] Moreover, molecular architecture has a dramatic effect on properties in PEG-based hydrogels.[36]

We have recently reported hydrogels with exceptionally dynamic character by exploiting telechelic block-like copolymers with self-complementary ureidopyrimidinone (UPy) units encapsulated within hydrophobic domains.[37−40] The hydrogels exhibited strong pH- and temperature-responsive gelation

Received: January 8, 2014
Published: May 6, 2014

   dx.doi.org/10.1021/ja500205v | J. Am. Chem. Soc. 2014, 136, 6969−6977

characteristics. However, under all conditions, these hydrogels were weak and brittle. Here, we expand upon this concept by preparing multiblock PEG-based copolymers having UPy moieties contained within the backbone. The mechanical properties are explored in both bulk (i.e., pristine) and hydrogel forms, clearly demonstrating the consequences of the multiblock, segmented molecular architecture (Figure 1).

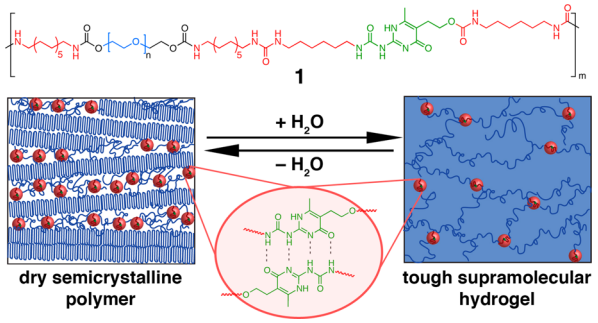

Figure 1. PEG-UPy chain-extended (co)polymers (**1**) with segmented multiblock architectures and self-complementary quadruple H-bonding interaction between two UPy segments; illustrative depiction of dry, semicrystalline polymer morphology and reversible transition to hydrogel upon water uptake.

Self-complementary UPy units assemble into strong dimers by four-fold hydrogen bonding (H-bonding), acting to reinforce networks,[41−43] while the noncovalent nature promotes processability, in contrast to chemical cross-links in conventional thermosets. The strength can additionally be adjusted by implementing different lengths/composition of PEG. This can be achieved in a straightforward manner by employing a modular synthetic protocol. The H-bonding motif allows phase-segregated segments to act as robust physical cross-links at relatively low composition. The integrity of cross-linking is maintained through molecular shielding with short-chain hydrophobic oligo-methylene spacers.[44,45] Combined with long PEG segments, this feature translates to low cross-link densities, allowing relatively large elongation−recovery to be achieved with minimal diminishment of modulus compared with pristine PEG. The cumulative mechanical properties are driven in part by the incompatibility between different chain segments (i.e., hydrophilic vs hydrophobic) in concert with the strong tendency for dimerization of the UPy motif.[42,43] A recent review highlights advances in the relatively new area of supramolecular hydrogels.[46] To our knowledge, few examples employ complementary H-bonding groups as physical cross-linkers in hydrogels.[15,47−49]

The implications of molecular architecture (i.e., chain-extended vs telechelic) were anticipated from the analogous chain-extended poly(ethylene-*s*-butene) with benzene tricarboxamide (BTA) groups in the backbone, which exhibited dramatically enhanced tensile toughness compared with the telechelic analogue.[50] The current work expands upon this notion by evaluating the tensile mechanical properties of **1** as a function of hydrophilic content across a range of temperatures and in both the hydrogel and pristine (i.e., dry) states.

RESULTS AND DISCUSSION

The multisegmented amphiphilic copolymers are prepared in a step-growth manner by reacting amino-telechelic PEG with diisocyanate functionalized UPy unit (see Figure S1 for the full synthetic scheme).[51] The synthetic protocol is modular; composition is tunable to enhance the strength and durability of the resulting hydrogels by employing different oligo-methylene spacers or different PEG chain lengths. To this end, chain-extended copolymers were prepared having a total of 36 methylene (CH_2) groups per macromolecular repeating unit (Figures 1 and S1; [−PEG_n−$C_{12}H_{24}$−Urea−C_6H_{12}−UPy−C_6H_{12}−Urea−$C_{12}H_{24}$−]). The effect of composition and PEG chain length was explored by preparing two samples having number-average molar mass (M_n) per PEG segment of either 6 or 10 kg mol^{-1}. These two different copolymers are referred to as **1-6k** and **1-10k** throughout, respectively.

The targeted end-group stoichiometry was 1:1 during the step-growth chain extension, ultimately providing samples with dramatically increased molecular weight and relatively broad molar mass distribution ($Đ$), as reflected by size exclusion chromatography (SEC) (Figure S2). Chain extension was performed in DMF; the polar solvent enabled high conversion by suppressing the UPy−UPy dimerization and therefore promoting solubility throughout the reaction, ultimately leading to very high molar mass. End-group conversion was monitored by ^{1}H NMR spectroscopy, in which the disappearance of signals associated with protons adjacent to the isocyanate and diamine precursors was followed (Figure S3). After precipitation into Et_2O, a white fluffy material was isolated; the chain-extended samples are then readily processable through melt-pressing or solvent casting (e.g., from methanol). We examined the structure development of the supramolecular aggregates formed and the mechanical properties of polymer **1** both in bulk and hydrogel states.

The modular synthetic features employed in this work are almost identical to that already reported, which allows tailoring of hydrophilicity and ductility by adjusting the composition through judicious choice of macromolecular building blocks. Extension of telechelic UPy−ABA−UPy copolymers to a segmented multiblock architecture −$(UPy−ABA)_n$− was recently demonstrated with various lengths of oligomeric methylene A-segments and different components for the B-segments (e.g., poly(ethylene-butene), poly(ethylene glycol).[49] The increased chain length realized through chain-extension substantially enhanced the strength, ductility, and stability in water for PEG-based copolymers compared with the telechelic analogues having nearly identical composition. We demonstrate the versatility of this synthetic approach in preparing tough hydrogels having tunable physical properties.

Thermal Analysis and Water Uptake. The strength embodied in the UPy−UPy dimers/aggregates can only be realized in strongly hydrophobic (e.g., nonprotic) environments.[37] The same principles apply to other supramolecular polymers that rely on H-bonding for self-assembly, such as benzene-1,3,5-tricarboxamides.[44,45,52−55] The amide functionality must be essentially shielded from hydrophilic environments in hybrid multicomponent systems. Network formation and mechanical performance therefore rest largely on retention of the physical cross-links across a range of temperatures and water content.

The melting transition of the PEG block in **1-10k** ($T_{m,PEG}$) occurs with a maximum in the heat flow profile at 56 °C and a melting enthalpy (ΔH_m = 95 J g^{-1}) corresponding to a normalized crystalline PEG fraction ϕ_x = 0.53 (Figure 2a).[56] The crystallinity and T_m are expectedly lower than pristine PEG having M_n = 10 kg mol^{-1}, as the confined chain architecture impedes crystallization (T_m = 62 °C; ΔH_m = 165−175 J g^{-1}; ϕ_x

dx.doi.org/10.1021/ja500205v | J. Am. Chem. Soc. 2014, 136, 6969−6977

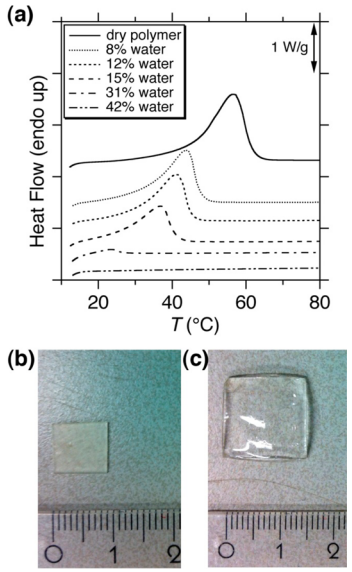

Figure 2. (a) DSC thermograms for the dry polymer **1** and hydrogels at various concentrations (second heating; 10 °C min^{-1}) and photographs of (b) melt-pressed film of dry polymer **1-10k** and (c) hydrogel from **1-10k** with 85 wt % water.

= 0.85−0.90). Likewise, crystallinity within polymer **1-10k** is notably less than the UPy-telechelic analogue (T_m = 56 °C; ΔH_m = 118−125 J g^{-1}; ϕ_x = 0.66−0.70), suggesting that less chain mobility occurs within the chain-extended sample, owing to the multiblock macromolecular architecture. This is consistent with a higher fraction of tethered PEG bridges between hydrophobic pockets in the multiblock chain-extended architecture compared with telechelic samples.[57−59] Bridging in microphase separated multiblock copolymers primarily serves to enhance tensile mechanical properties.

Samples **1-10k** and **1-6k** contain PEG weight fractions (w_{PEG}) of 0.93 and 0.90, respectively. The large proportion of PEG resulted in extensive water uptake. Hydrophobic segments phase separate from the hydrophilic PEG, and thereby a physically cross-linked system arises at relatively low polymer concentrations.[37] However, in the limit of infinite dilution, films consisting of polymers **1-10k** or **1-6k** do not dissolve molecularly in water at 25 °C. In contrast, the films absorb an equilibrium water content and retain the original shape of the dried film, albeit swollen in all dimensions. At equilibrium at ambient temperature, hydrogels from polymers **1-10k** and **1-6k** contain water weight fractions (w_{H2O}) of 0.86 and 0.81, respectively. The water can subsequently be removed, and the film can be redissolved in methanol for further processing or reswelled in water. The hydrogels can therefore be generated in a reversible manner. All chains within the sample carry UPy segments that participate in network formation. There was no measurable mass loss after soaking the films at concentration <0.1 mg/mL for longer than 30 days. Water is selectively absorbed into the PEG domains, gradually dislodging increasing amounts of lattice-organized chain segments from crystalline regions with increasing water content, as evident from differential scanning calorimetry (DSC) thermograms of polymer **1-10k** with various water content (Figure 2a). Eventually (at ca. 42 wt % water), the material is essentially completely amorphous. Soaking the polymer **1-10k** and **1-6k** in very dilute solutions at ambient temperature leads to an eventual equilibrium degree of swelling and a transparent sample, illustrated for polymer **1-10k** with 85 wt % water and 86 vol % increase (Figure 2b,c). The insolubility presumably arises from the physical cross-links, which are maintained in the hydrophilic hydrogel environment despite the reliance on H-bonding between UPy groups. This suggests that the hydrophobic methylene spacers effectively shield the UPy and facilitate aggregation such that H-bonding disruption/dissociation caused by the hydrated matrix is prevented. This observation is consistent with a microphase separated, physically cross-linked system as opposed to a compositionally homogeneous sample merely having very high molecular mass. In fact, PEG with molar mass of 5 000 000 g mol^{-1} is still water-soluble at ambient temperature; stable hydrogels are not formed (at >80 wt % water) despite the astronomical chain length (>100 000 repeating units). There is no evidence for higher ordered structures in the dry or hydrated state for the chain-extended polymers **1**; melting of aggregated UPy dimers in extended fibrous structures was not observed by DSC.[60]

Nanoscale Morphology. Analyses of material properties of hydrogels are often used as indirect evidence of the envisioned material superstructure or morphological architecture. However, recent advancements in cryo-electron microscopy and high-sensitive direct-electron detectors made it possible to directly image the dry, gelled, and intermediate states at nanometer resolution. With this technique it is possible to distinguish between the hydrophobic and hydrophilic domains and between (semi)-crystalline and amorphous regions based on the natural electron-density contrast; selective staining is unnecessary.

Development of a physical network morphology during hydration should generate materials with microphase segregated domains, owing to the thermodynamic immiscibility between segments. Cryo-transmission electron microscopy (cryo-TEM) and environmental scanning electron microscopy (ESEM) allowed us to obtain a glimpse of the nanoscale morphology *in situ* during the transition from bulk (i.e., dry material) to a hydrogel. High-resolution imaging techniques ultimately suggest that nanometer-scale phase separation persists across a broad spectrum of conditions (Figure 3a−c). TEM micrographs of dry polymer **1-10k** show a predominantly lamellar morphology composed of alternating crystalline and amorphous PEG segments (Figure 3a), consistent with the relatively high crystalline content indicated by DSC (Figure 2) and wide-angle X-ray scattering (WAXS) (Figure 4a). The lamellar thickness measured by TEM is ∼15 nm, consistent with previously measured periodicities for pure PEG of similar molecular weight and large super cooling.[61,62]

Using an ESEM equipped with a scanning transmission electron microscopy (STEM) detector (see Supporting Information for detailed instrument description), the materials can be imaged at high resolution under high humidity conditions. Therefore, the gelation process was monitored, and structure evolution at nanometer length scale was observed. Micrographs during hydration suggest that the hydrophobic segments segregate into nanoscale domains and preferentially occupy the interstitial amorphous volume between crystalline PEG lamellae throughout the hydration process (Figure 3b). This heterogeneous segregation is expected in the dry material as crystalline PEG segments expel the incompatible hydrophobic domains during crystallization into the tightly packed monoclinic lattice. Small (<5 nm) spherical compartments are observed between the crystalline lamellae (Figure 3a,b) as illustrated schematically

dx.doi.org/10.1021/ja500205v | J. Am. Chem. Soc. 2014, 136, 6969−6977

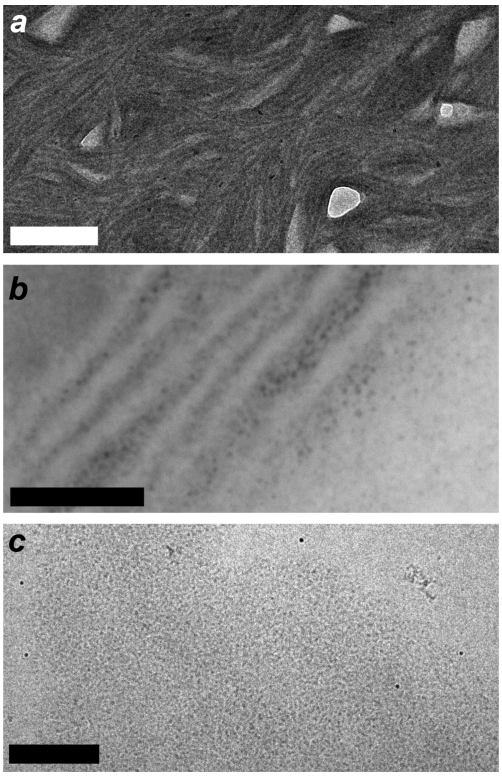

Figure 3. Micrographs showing the morphological characteristics of the polymer **1** (with 10 kg mol^{-1} PEG segments) in various states: (a) cryo-TEM image of dry material after casting directly onto grid, showing semicrystalline, lamellar morphology −200 nm scale bar; (b) STEM image of partially hydrated material upon in situ gradual humidity increase, showing domains of various length scales −50 nm scale bar; (c) cryo-TEM micrograph of fully hydrated material showing dense dispersion of darker spherical domains −200 nm scale bar.

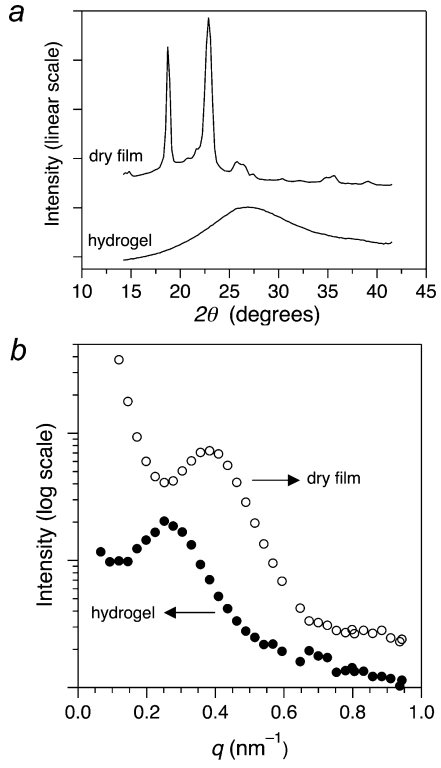

Figure 4. (a) WAXS and (b) SAXS results for the dry material and hydrogel of polymer **1-10k**.

in Figure 1. We contend that the crystalline regions preferentially absorb water faster than the layers enriched in hydrophobic pockets. Therefore, Figure 3b shows a lighter contrast in the layers that are deficient in denser hydrophobic compartments. Low vacuum conditions were exploited to probe the morphological evolution with increasing water content, during which the crystalline lamellae undergo gradual dissolution as humidity is increased during imaging (Figure 3b,c). Lamellae associated with the crystallites diminish in intensity as water is absorbed, and the PEG phase becomes homogeneous.

Ultimately upon complete transition to a hydrogel state, TEM micrographs reveal a nearly homogeneous light matrix consisting of the amorphous hydrated PEG (Figure 3c). We attribute the tiny darker spherical features to small hydrophobic domains comprising UPy−UPy dimers flanked by the dense oligo-methylene segments (Figure S4). The hydrophobic segments effectively shield the water from disrupting the H-bonding, upon which UPy dimerization depends. Somewhat unexpectedly, the hydrophobic segments appear to be dispersed as small spherical compartments with ∼2−5 nm diameter.

Small-angle X-ray scattering (SAXS) measurements performed in dry and hydrated states further suggest that microphase separation persists under both conditions (Figure 4b). A single, broad scattering reflection in the one-dimensional plot indicates a disorganized dispersion of phase-separated objects with an average spacing of ∼16.5 nm (according to spacing $d = 2\pi/q$, where $q = 4\pi\,\lambda^{-1}\sin\theta$). After swelling, the domain spacing is increased to 23.8 nm, consistent with selective swelling in the PEG domain and retention of the hydrophobic domains that comprise the physical cross-links. Neither the dry material nor the hydrogel exhibit scattering associated with crystallinity in the oligo-methylene segments (Figure 4a). The diffraction pattern is consistent with a monoclinic crystal structure adopted by PEG.[63] Microphase separation is likely driven by a hydrophobic effect; however, the physical cross-linking and mechanical stability stems primarily from UPy−UPy aggregation as opposed to crystallization.

The morphology adopted by polymer **1** must contain a large portion of bridged PEG segments connecting the dispersed hydrophobic compartments as a natural consequence of the molecular architecture. The ramifications of this network morphology and composition should be expressed by mechanical resilience. Furthermore, the performance of the materials and stability of the physical cross-links in various temperature regimes is of great interest, both in the pristine and hydrated states.

Mechanical Performance. Dynamic mechanical analysis of the polymer **1-10k** shows a precipitous decrease (2 orders of magnitude) in both storage and loss moduli (E' and E'', respectively) over a narrow temperature range of 50−60 °C (Figure 5a). Polymer **1-6k** has essentially identical response (Figure S5). The indicated T_{trans} corresponds with $T_{m,PEG}$ measured by DSC. The mechanical response indicates predominantly elastic behavior ($E' \gg E''$) over the entire temperature range (20−140 °C). The hydrophobic domains with strongly self-associated UPy units and high proportions of interconnected PEG network (i.e., bridging) are responsible for the elastic behavior well above $T_{m,\,PEG}$, with E' maintained in the range 1−3 MPa from 140−70 °C. This is directly

dx.doi.org/10.1021/ja500205v | J. Am. Chem. Soc. 2014, 136, 6969−6977

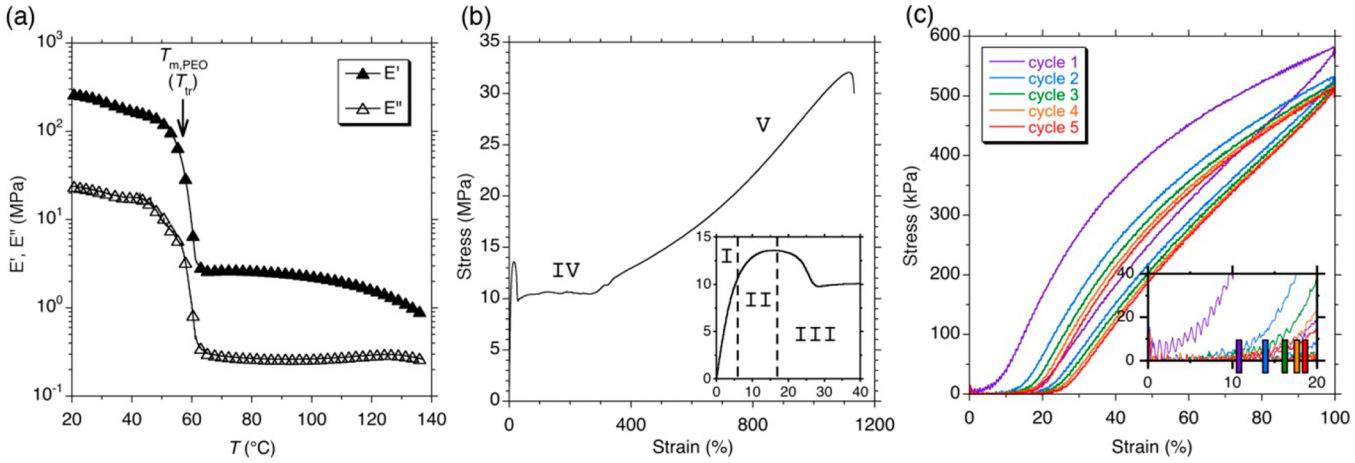

Figure 5. (a) Temperature-dependent storage modulus (E') and loss modulus (E'') for chain-extended UPy–PEG polymer **1-10k** (1 Hz; 3 °C min^{-1}). (b) Tensile testing results for pristine, dry polymer **1-10k** at ambient temperature with an inset to show yielding and onset of cold-drawing. (c) Cyclic tensile testing at 70 °C (5 cycles each having maximum strain ε_{max} = 100%) and the inset illuminating the residual strain after the first elongation.

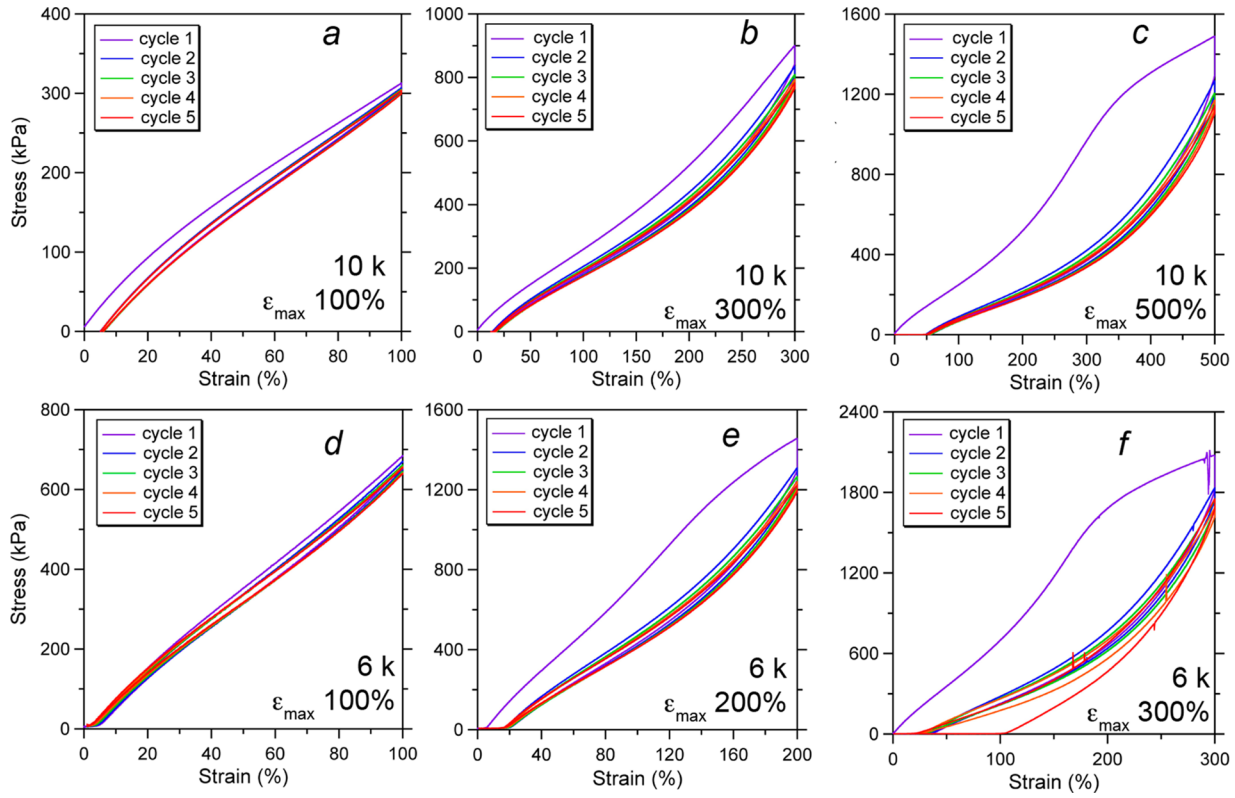

Figure 6. Cyclic stress–strain results for hydrogels from polymer **1-10k** with maximum strain (ε_{max}) of (a) 100%, (b) 300%, and (c) 500% and hydrogels from polymer **1-6k** with ε_{max} of (d) 100%, (e) 200%, and (f) 300% having 5 cycles each.

comparable to the modulus observed in shape memory polymers comprising poly(methyl acrylate), poly(methyl methacrylate), and poly(isobornyl acrylate) mixtures.[34] However, our single-component system offers appealing conceptual simplicity for achieving a similar rubbery modulus.

The contrasting behavior in the different temperature regimes for polymer **1** was explored with uniaxial elongation, which reveals a strong ductile material at ambient temperature (Figure 5b; Young's modulus, E = 234 ± 6 MPa). Chain-extended polymer **1** is exceptionally ductile (**1-10k**, work of extension W_e = 193 ± 12 J cm^{-3}) and exhibits profoundly different bulk mechanical characteristics than the purely telechelic analogue, implicating the importance of the chain architecture in accessing increased toughness (see Figure S6 for tensile test of telechelic polymer). Maximum elongation before fracture was consistently more than 10-fold the original length of polymer **1-10k** and **1-6k**, with an average yield strength (σ_{yld}) of 13 MPa (Figure 5b). The strong incompatibility of the two components (UPy vs PEG) allows very low hydrophobic content (e.g., **1-10k** w_{PEG} = 0.92), whereby the modulus is only modestly depressed compared with pristine PEG (5000 kg mol^{-1}; E = 285 ± 7 MPa; see Figure S7). Representative

dx.doi.org/10.1021/ja500205v | J. Am. Chem. Soc. 2014, 136, 6969–6977

stress−strain curve for polymer **1-10k** at ambient temperature highlights the various responses associated with the macroscopic deformation mechanism (Figure 5b; engineering stress = F/A_0 [force divided by initial cross-sectional area]). Region I is characterized by a steep incline that reflects the relatively high Young's modulus. The sample yields (Region II) and begins to neck at ∼10% strain, marked by a decrease in the stress resulting from smaller cross-sectional area than the original, undeformed gauge (Region III). The sample is subsequently cold drawn (Region IV) as the neck propagates throughout the gauge length, during which stress is essentially constant. The strength continuously increases after the neck has completely propagated the gauge, whereby the sample undergoes strain hardening with a stress increase (Region V) until failure at ∼1100% strain. The cumulative results from the tensile test indicate a tough material despite the relatively low UPy−hydrophobic content.

The chain-extended polymer **1** exhibits elastic behavior above $T_{m,PEG}$. Resilience was probed with cyclic tensile testing at elevated temperature (T = 70 °C > $T_{m,PEG}$) (Figure 5c). The sample became transparent upon heating, suggesting an amorphous microphase separated morphology. Uniaxial extension was applied to 100% strain followed by returning to the original gauge length. This cycle was repeated five times, and the hysteresis can be measured by the ratio of work of extension (W_e; area under the stress−strain curve) on the first elongation to the work of subsequent cycles (W_N; N = cycle number). Figure 5c indicates that when the maximum strain (ε_{max}) is 100%, there is noticeable hysteresis and residual strain of ∼10% on the second cycle (see inset of Figure 5c). The hysteresis suggests energy dissipation, which was not reversible and likely due to covalent breakage of PEG chains. Nonetheless, the sample is resilient, despite being above the $T_{m,PEG}$ and being completely amorphous. The elasticity above $T_{m,PEG}$ is likely a direct consequence of the morphological features indicated by TEM, whereby UPy−UPy dimers are maintained and consequently act to reinforce the hydrophobic physical cross-links to form thermoplastic elastomeric materials.[60]

The network retention upon hydration was also probed by cyclic tensile testing on hydrogels from polymers **1-10k** and **1-6k** (see Supporting Information for sample preparation protocol). As with the elevated temperature measurements, dog-bones were subjected to uniaxial elongation to various values of ε_{max} followed by returning to the original position. Identical cycles were repeated five times, and the resilience was evaluated while measuring the forces associated with deformation (Figure 6). The ultimate stress at 100% elongation for hydrogel **1-10k** was ∼30× lower than the dry sample at ambient temperature and 1.5× lower than the dry sample at 70 °C (Figure 6a). However, the sample exhibited only minor hysteresis from the first to the second cycle and showed nearly perfect recovery during each subsequent cycle. Excellent recovery was also observed for higher ultimate elongation (e.g., 300% in Figure 6b). After the first cycle, somewhat larger hysteresis was observed; each subsequent cycle had essentially perfect recovery. The recovery profile is consistent with a material having exceptionally stable physical cross-links that are retained in the presence of high-water content and under strenuous mechanical deformation. The physical cross-linking of the hydrogel is also maintained at elevated temperature, as evident by the relatively temperature- and frequency-independent modulus measured by rheology (Figure S8). Extending to ε_{max} of 500% in the cyclic tensile tests shows considerably larger hysteresis and irreparable damage between cycles 1 and 2. Again, the recovery on subsequent cycles improves dramatically.

Hydrogels of sample **1-6k** demonstrate a similar trend with respect to ε_{max} and irreparable damage (Figure 6d−f). However, there are noteworthy differences. First, at a given value of ε_{max} (e.g., 100% or 300%), the ultimate stress is substantially higher (two-fold) for polymer **1-6k** than for **1-10k**. Likewise, the hysteresis becomes more prominent at lower ε_{max} for polymer **1-6k** than for **1-10k**. The hysteresis and resilience can be reflected by the ratio $W_N/W_{N=1}$, shown for the two hydrogel samples in Figure 7 as a function of cycle number N.

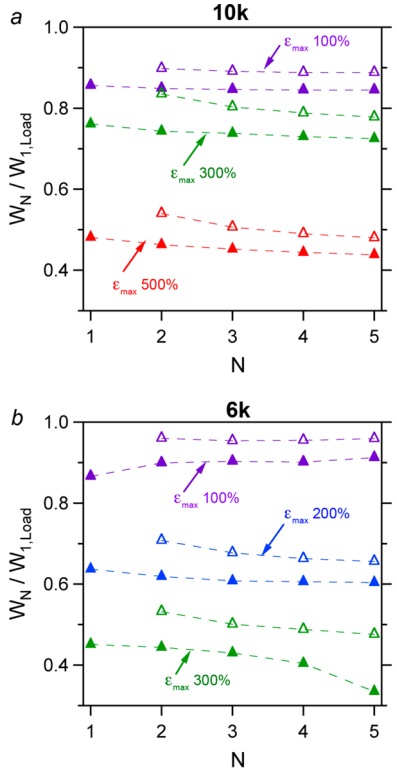

Figure 7. Resilience of the hydrogel materials reflected by the ratio of work (W_N) of subsequent loadings (unfilled triangles) and unloadings (filled triangles) to the work of the first loading ($W_{N=1,Load}$) for the hydrogels formed from polymers (a) **1-10k** and (b) **1-6k**.

The results clearly indicate that hydrogels of polymer **1-10k** undergo less irreparable damage at a given extension length. This suggests that during deformation/elongation, the PEG chains are stretched in the water matrix until they reach a maximum value. Having been essentially stretched taut, chains begin to fracture, causing irrecoverable damage. The broken chains no longer contribute to the strength of the materials, and when stretched again, they exhibit almost identical mechanical characteristics. Consequently, the extension value at which an appreciable chain rupture occurs is directly proportional to the PEG chain length. Additionally, shorter chains correspond to higher cross-link density and thus higher stress, as seen in a comparison of the two polymers **1-10k** and **1-6k** (Table 1).[64]

We hypothesize that the physical cross-links in this system benefit greatly from the H-bonding UPy motif and not solely from a hydrophobic effect. For example, the mechanical profile is substantially stronger and tougher than hydrogels formed by chemically cross-linked copolymer micelles with very similar

dx.doi.org/10.1021/ja500205v | J. Am. Chem. Soc. 2014, 136, 6969−6977

Table 1. Mechanical Properties of Hydrogels from Polymers 1-10k and 1-6k at Various Elongations

			cycle 1	
sample	ε_{max} (%)	σ_{max} (MPa)	W_{Load} (J cm^{-3})	W_{Unload} (J cm^{-3})
1-10k	100	0.31	0.18	0.15
1-10k	300	0.90	1.23	0.94
1-10k	500	1.49	3.80	1.83
1-6k	100	0.68	0.35	0.30
1-6k	200	1.45	1.51	0.96
1-6k	300	2.07	3.44	1.55

composition (i.e., hydrophobic vs hydrophilic content).[65−68] Furthermore, the absence of chemical cross-links in our multisegment chain extended polymers offers attractive processing opportunities and reversible hydrogel formation. The materials are ideal for further investigation into fracture mechanism in hybrid hydrogels.

Shape Memory Behavior. Shape memory polymers (SMPs) are a subset of resilient materials, where the crucial feature is the control over the chain conformations and dynamics under various conditions. After macroscopic deformation from an equilibrium (i.e., permanent) shape, the temporary shape should be retained until a controlled stimulus (e.g., heat, light,[69−72] solvent exposure[73]) induces recovery to the original geometry.[74,75] The permanent molecular structure typically consists of a deformable soft matrix with either physical or chemical cross-links defining an equilibrium conformation. Shape recovery is driven by the entropic gain from chain relaxation, which is accelerated appreciably above T_g or T_m. Specifically, biocompatible synthetic polymers with shape memory behavior hold tremendous promise for critically important applications in the biomedical industry, including sutures and implantable stents.[76−80] These polymers must be strong, durable, and resilient, preferably under a range of conditions, including physiological (e.g., hydrated, elevated temperature, cell presence).[81]

The thermal/mechanical profile of the materials described here was exploited for shape memory behavior. The melting transition occurs over a relatively narrow temperature range, which is typical of SMPs that employ semicrystalline switching domains.[82] Polymer **1-10k** was formed into a permanent shape by two methods, evidence of the relative ease of processability. The polymer was dissolved in methanol and cast as a film (ca. 0.5 mm thickness). Alternatively the polymer was pressed into a film at 120 °C. Either straight strips or curved "S" shapes were cut from the films, representing the permanent geometries.

The hydrophilicity of PEG lent itself toward an alternative stimulus to induce recovery to a permanent shape, which was previously demonstrated for networks having a hydrophilic matrix. However, this could only occur if the complementary H-bonding between UPy groups remains intact while hydrated, as suggested by the mechanical properties.

Two alternative stimuli were demonstrated: heat and water. The permanent "S"-shaped samples were heated to 70 °C. The samples were then straightened (mechanical deformation by hand), followed by cooling to ambient temperature, which effectively fixed this temporary shape upon crystallization of the matrix phase. The samples become visibly transparent upon heating, and subsequent cooling caused increased opacity owing to crystallization. The straightened temporary shape was then submerged in a nonsolvent at 70 °C, and the shape recovery was monitored visually with digital photography (Figure 8a). Thermally activated shape recovery occurred rapidly, fully reverting to the permanent shape within 10 s when the fluid was silicon oil. An alternative nonsolvent, heptane, was also shown to activate the recovery process very quickly (<5 s; see Figures 8c and S9 and Supporting Information video V1). The recovery was attributed solely to the thermal contribution; the mass of the sample was equal before and after the recovery experiment, and the polymer constituents are highly immiscible in hydrocarbons like heptane. Submergence in liquid was used to aide in visualization of the very fast recovery process. Furthermore, samples exhibited recovery from various types of deformation. For example, a sample was subjected to uniaxial extension at ambient temperature to ∼200% strain. The samples retain this temporary shape indefinitely. Substantial whitening is observed upon extension, as with all the other samples having undergone tensile testing (Figure 8c). When submerged in heptane at 70 °C, the sample nearly instantaneously contracts back to the original dimensions (Supporting Information video V2).

Submerging a sample in the temporary shape in water at ambient temperature shares some behavioral qualities with

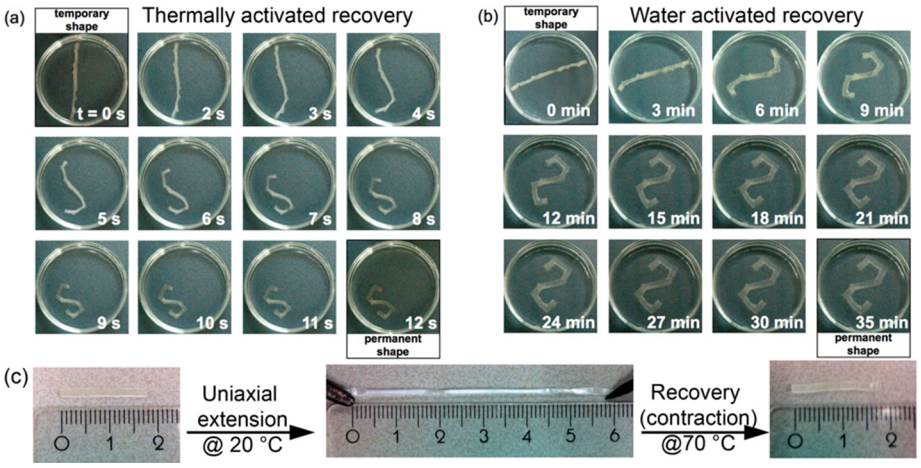

Figure 8. Shape memory behavior observed in response to (a) thermally activated phase transition ($T_{trans} = T_{m,PEG}$) in silicone oil at 70 °C; (b) water activated phase transition during hydrogel formation at 20 °C; (c) thermally activated phase transition from uniaxially extended polymer ($\Delta L/L_0 \approx 2$) from submerging in heptane at 70 °C.

dx.doi.org/10.1021/ja500205v | J. Am. Chem. Soc. 2014, 136, 6969−6977

thermally activated shape recovery. The temporary straightened shape (Figure 8b, t = 0 min) was initially opaque and became gradually transparent as water was absorbed. The permanent shape was gradually recovered as the water diffused completely into the structure and crystallinity was correspondingly suppressed. Notably, the recovery process was much slower than the thermally induced transition (at 70 °C), requiring more than 15 min to recover. As a natural consequence of the hydrophilicity, the recovery was also accompanied by swelling to the eventual equilibrium water content (ca. 90 wt % water). The diffusion of heat through the materials appears to be substantially faster than water, as expected. However, the results are consistent with a material being multiply responsive toward shape recovery. Each pathway could foreseeably lend itself to certain technologically demanding biomaterials.

CONCLUSIONS

We have described the preparation of hybrid materials comprising a hydrophilic PEG matrix combined with nanoscopic hydrophobic compartments with associative strength amplified by hydrogen-bonded motifs. Unique imaging techniques that allow high resolution capture in a low-vacuum/high-humidity environment helped elucidate the unexpected morphologies in pristine and hydrated states. Tensile testing under various conditions revealed a remarkably strong hydrogel that exhibits nearly perfect strength recovery even at large deformation (>300%). The mechanical properties of the multicomponent segmented copolymers at ambient temperature coupled with the strong hydrophilicity embodied by the high PEG content offer enticing opportunities for exploration. These polymers may be ideally suited for applications requiring high strength and flexibility in tandem with lithium salt compatibility, e.g., as lithium-ion battery solid electrolytes. Furthermore, the modular synthetic strategy employed facilitates straightforward tailoring of the physical properties, such that optimal performance can be targeted for various applications. The biocompatibility of the PEG also presents appealing avenues for use in the biomedical arena, such as adaptive sutures, flexible stents, and tissue engineering. Likewise, we are actively exploring the combination of the chain-extended polymers with the previously reported telechelic UPy–PEG hybrids with the aim of finely tuning the hydrogel dynamics and stability. Collectively, these polymers embody many of the characteristics that are sought in various fields. They provide progress toward addressing the challenges of achieving structural simplicity married with sophisticated dynamic and responsive behavior. We envision exploring the possibilities of tailoring swelling ratios and thermal transition temperatures through tuning the matrix constituents and composition. We propose that the biomedical (polymer) market could benefit tremendously from a simple, single component, easily processable, molecularly dynamic, biocompatible shape memory polymer, such as that described in this article.

ASSOCIATED CONTENT

Supporting Information

Experimental details, electron micrographs, SEC, ^{1}H NMR spectra, tensile tests, digital photographs, and movies from shape memory behavior. This material is available free of charge via the Internet at http://pubs.acs.org.

AUTHOR INFORMATION

Corresponding Author

e.w.meijer@tue.nl

Author Contributions

[#]These authors contributed equally.

Notes

The authors declare no competing financial interest.

ACKNOWLEDGMENTS

We thank Donglin Tang, Bram Pape, and Ilja Voets for helping in data collection efforts. The authors are grateful for funding through NRSC-C. The research leading to these results has received funding from the Ministry of Education, Culture and Science (Gravity program 024.001.035), The Netherlands Organization for Scientific Research (NWO), and the European Research Council (FP7/2007-2013) ERC Grant Agreement 246829. This research forms part of the Project P1.03 PENT of the research program of the BioMedical Materials institute, cofunded by the Dutch Ministry of Economic Affairs.

REFERENCES

(1) Gupta, P.; Vermani, K.; Garg, S. *Drug Discovery Today* **2002**, *7*, 569.
(2) Jagur-Grodzinski, J. *Polym. Adv. Technol.* **2006**, *17*, 395.
(3) Peppas, N. A.; Hilt, J. Z.; Khademhosseini, A.; Langer, R. *Adv. Mater.* **2006**, *18*, 1345.
(4) Yoshida, M.; Langer, R.; Lendlein, A.; Lahann, J. *Polym. Rev.* **2006**, *46*, 347.
(5) Chaterji, S.; Kwon, I. K.; Park, K. *Prog. Polym. Sci.* **2007**, *32*, 1083.
(6) Yu, L.; Ding, J. *Chem. Soc. Rev.* **2008**, *37*, 1473.
(7) Kopecek, J. *J. Polym. Sci., Part A: Polym. Chem.* **2009**, *47*, 5929.
(8) Mohammed, J. S.; Murphy, W. L. *Adv. Mater.* **2009**, *21*, 2361.
(9) Slaughter, B. V.; Khurshid, S. S.; Fisher, O. Z.; Khademhosseini, A.; Peppas, N. A. *Adv. Mater.* **2009**, *21*, 3307.
(10) Lee, K. Y.; Mooney, D. J. *Chem. Rev.* **2001**, *101*, 1869.
(11) Tanaka, Y.; Gong, J. P.; Osada, Y. *Prog. Polym. Sci.* **2005**, *30*, 1.
(12) Peak, C. W.; Wilker, J. J.; Schmidt, G. *Colloid Polym. Sci.* **2013**, *291*, 2031.
(13) Lange, R. F. M.; Van Gurp, M.; Meijer, E. W. *J. Polym. Sci., Part A: Polym. Chem.* **1999**, *37*, 3657.
(14) Liu, G. Q.; Guan, C. L.; Xia, H. S.; Guo, F. Q.; Ding, X. B.; Peng, Y. X. *Macromol. Rapid Commun.* **2006**, *27*, 1100.
(15) Li, J.; Viveros, J. A.; Wrue, M. H.; Anthamatten, M. *Adv. Mater.* **2007**, *19*, 2851.
(16) Fan, M. M.; Yu, Z. J.; Luo, H. Y.; Sheng, Z.; Li, B. J. *Macromol. Rapid Commun.* **2009**, *30*, 897.
(17) Doring, A.; Birnbaum, W.; Kuckling, D. *Chem. Soc. Rev.* **2013**, *42*, 7391.
(18) White, E. M.; Yatvin, J.; Grubbs, J. B.; Bilbrey, J. A.; Locklin, J. *J. Polym. Sci., Part B: Polym. Phys.* **2013**, *51*, 1084.
(19) Hao, J.; Weiss, R. A. *ACS Macro Lett.* **2013**, *2*, 86.
(20) Lendlein, A.; Shastri, V. P. *Adv. Mater.* **2010**, *22*, 3344.
(21) Sun, J.-Y.; Zhao, X.; Illeperuma, W. R. K.; Chaudhuri, O.; Oh, K. H.; Mooney, D. J.; Vlassak, J. J.; Suo, Z. *Nature* **2012**, *489*, 133.
(22) Ducrot, E.; Chen, Y.; Bulters, M.; Sijbesma, R. P.; Creton, C. *Science* **2014**, *344*, 186.
(23) Zhao, X. *Soft Matter* **2014**, *10*, 672.
(24) Wang, M. T.; Luo, X. L.; Zhang, X. Y.; Ma, D. Z. *Polym. Adv. Technol.* **1997**, *8*, 136.
(25) Wang, M. T.; Luo, X. L.; Ma, D. Z. *Eur. Polym. J.* **1998**, *34*, 1.
(26) Chen, W.; Zhu, C. Y.; Gu, X. R. *J. Appl. Polym. Sci.* **2002**, *84*, 1504.
(27) Liu, G. Q.; Ding, X. B.; Cao, Y. P.; Zheng, Z. H.; Peng, Y. X. *Macromolecules* **2004**, *37*, 2228.
(28) Chung, Y. C.; Cho, T. K.; Chun, B. C. *J. Appl. Polym. Sci.* **2009**, *112*, 2800.

(29) Inomata, K.; Nakagawa, K.; Fukuda, C.; Nakada, Y.; Sugimoto, H.; Nakanishi, E. *Polymer* **2010**, *51*, 793.
(30) Li, J.; Liu, T.; Xia, S.; Pan, Y.; Zheng, Z. H.; Ding, X. B.; Peng, Y. X. *J. Mater. Chem.* **2011**, *21*, 12213.
(31) Grijpma, D. W.; Feijen, J. *J. Controlled Release* **2001**, *72*, 247.
(32) Guo, C.; Bailey, T. S. *Soft Matter* **2010**, *6*, 4807.
(33) Bates, F. S.; Fredrickson, G. H. *Phys. Today* **1999**, *52*, 32.
(34) Voit, W.; Ware, T.; Dasari, R. R.; Smith, P.; Danz, L.; Simon, D.; Barlow, S.; Marder, S. R.; Gall, K. *Adv. Funct. Mater.* **2010**, *20*, 162.
(35) Sun, T. L.; Kurokawa, T.; Kuroda, S.; Ihsan, A. B.; Akasaki, T.; Sato, K.; Haque, M. A.; Nakajima, T.; Gong, J. P. *Nat. Mater.* **2013**, *12*, 932.
(36) Sakai, T.; Matsunaga, T.; Yamamoto, Y.; Ito, C.; Yoshida, R.; Suzuki, S.; Sasaki, N.; Shibayama, M.; Chung, U.-i. *Macromolecules* **2008**, *41*, 5379.
(37) Dankers, P. Y. W.; Hermans, T. H.; Baughman, T. W.; Kamikawa, Y.; Kieltyka, R. E.; Bastings, M. M. C.; Janssen, H. M.; Sommerdijk, N. A. J. M.; Larsen, A.; van Luyn, M. J. A.; Popa, E. R.; Bosman, A. W.; Fytas, G.; Meijer, E. W. *Adv. Mater.* **2012**, *24*, 2703.
(38) Bastings, M. M. C.; Koudstaal, S.; Kieltyka, R. E.; Nakano, Y.; Pape, A. C. H.; Feyen, D. A. M.; van Slochteren, F. J.; Doevendans, P. A.; Sluijter, J. P. G.; Meijer, E. W.; Chamuleau, S. A. J.; Dankers, P. Y. W. *Adv. Healthcare Mater.* **2013**, *3*, 70.
(39) Kieltyka, R. E.; Pape, A. C. H.; Albertazzi, L.; Nakano, Y.; Bastings, M. M. C.; Voets, I. K.; Dankers, P. Y. W.; Meijer, E. W. *J. Am. Chem. Soc.* **2013**, *135*, 11159.
(40) Pape, A. C. H.; Bastings, M. M. C.; Kieltyka, R. E.; Wyss, H. M.; Voets, I. K.; Meijer, E. W.; Dankers, P. Y. W. *Int. J. Mol. Sci.* **2014**, *15*, 1096.
(41) Sontjens, S. H. M.; Sijbesma, R. P.; van Genderen, M. H. P.; Meijer, E. W. *J. Am. Chem. Soc.* **2000**, *122*, 7487.
(42) Beijer, F. H.; Sijbesma, R. P.; Kooijman, H.; Spek, A. L.; Meijer, E. W. *J. Am. Chem. Soc.* **1998**, *120*, 6761.
(43) Folmer, B. J. B.; Sijbesma, R. P.; Versteegen, R. M.; van der Rijt, J. A. J.; Meijer, E. W. *Adv. Mater.* **2000**, *12*, 874.
(44) de Greef, T. F. A.; Nieuwenhuizen, M. M. L.; Stals, P. J. M.; Fitie, C. F. C.; Palmans, A. R. A.; Sijbesma, R. P.; Meijer, E. W. *Chem. Commun.* **2008**, 4306.
(45) Stals, P. J. M.; Haveman, J. F.; Martin-Rapun, R.; Fitie, C. F. C.; Palmans, A. R. A.; Meijer, E. W. *J. Mater. Chem.* **2009**, *19*, 124.
(46) Appel, E. A.; Barrio, J. d.; Loh, X. J.; Scherman, O. A. *Chem. Soc. Rev.* **2012**, *41*, 6195.
(47) Ware, T.; Hearon, K.; Lonnecker, A.; Wooley, K. L.; Maitland, D. J.; Voit, W. *Macromolecules* **2012**, *45*, 1062.
(48) Cui, J.; Campo, A. d. *Chem. Commun.* **2012**, *48*, 9302.
(49) Gemert, G. M. L. v.; Peeters, J. W.; Söntjens, S. H. M.; Janssen, H. M.; Bosman, A. W. *Macromol. Chem. Phys.* **2012**, *213*, 234.
(50) Roosma, J.; Mes, T.; Leclere, P.; Palmans, A. R. A.; Meijer, E. W. *J. Am. Chem. Soc.* **2008**, *130*, 1120.
(51) Söntjens, S. H. M.; Renken, R. A. E.; van Gemert, G. M. L.; Engels, T. A. P.; Bosman, A. W.; Janssen, H. M.; Govaert, L. E.; Baaijens, F. P. T. *Macromolecules* **2008**, *41*, 5703.
(52) Besenius, P.; Portale, G.; Bomans, P. H. H.; Janssen, H. M.; Palmans, A. R. A.; Meijer, E. W. *Proc. Natl. Acad. Sci. U. S. A.* **2010**, *107*, 17888.
(53) Besenius, P.; van den Hout, K. P.; Albers, H.; de Greef, T. F. A.; Olijve, L. L. C.; Hermans, T. M.; de Waal, B. F. M.; Bomans, P. H. H.; Sommerdijk, N.; Portale, G.; Palmans, A. R. A.; van Genderen, M. H. P.; Vekemans, J.; Meijer, E. W. *Chem.—Eur. J.* **2011**, *17*, 5192.
(54) Terashima, T. T. T.; Mes, T.; De Greef, T. F. A.; Gillissen, M. A. J.; Besenius, P.; Palmans, A. R. A.; Meijer, E. W. *J. Am. Chem. Soc.* **2011**, *133*, 4742.
(55) Leenders, C. M. A.; Albertazzi, L.; Mes, T.; Koenigs, M. M. E.; Palmans, A. R. A.; Meijer, E. W. *Chem. Commun.* **2013**, *49*, 1963.
(56) Calculated by $\Pi_{PEG} = \Delta H_m/(\Delta H_m^0 \cdot w_{PEG})$ where w_{PEG} = weight fraction of PEG in the sample and ΔH_m^0 (heat of fusion at 100% crystallinity) is taken at 196.6 J g^{-1} from: Qiu, W.; Wunderlich, B. *Thermochim. Acta* **2006**, *448*, 136.
(57) Matsen, M. W. *J. Chem. Phys.* **1995**, *102*, 3884.
(58) Phatak, A.; Lim, L. S.; Reaves, C. K.; Bates, F. S. *Macromolecules* **2006**, *39*, 6221.
(59) Drolet, F.; Fredrickson, G. H. *Macromolecules* **2001**, *34*, 5317.
(60) Kautz, H.; van Beek, D. J. M.; Sijbesma, R. P.; Meijer, E. W. *Macromolecules* **2006**, *39*, 4265.
(61) Cheng, S. Z. D.; Bu, H. S.; Wunderlich, B. *J. Polym. Sci., Part B: Polym. Phys.* **1988**, *26*, 1947.
(62) Leggett, G. J.; Wilkins, M. J.; Davies, M. C.; Jackson, D. E.; Roberts, C. J.; Tendler, S. J. B. *Langmuir* **1993**, *9*, 1115.
(63) Qiu, W.; Pyda, M.; Nowak-Pyda, E.; Habenschuss, A.; Wunderlich, B. *J. Polym. Sci., Part B: Polym. Phys.* **2007**, *45*, 475.
(64) Yazici, I.; Okay, O. *Polymer* **2005**, *46*, 2595.
(65) Abdurrahmanoglu, S.; Can, V.; Okay, O. *Polymer* **2009**, *50*, 5449.
(66) Abdurrahmanoglu, S.; Cilingir, M.; Okay, O. *Polymer* **2011**, *52*, 694.
(67) Tuncaboylu, D. C.; Sari, M.; Oppermann, W.; Okay, O. *Macromolecules* **2011**, *44*, 4997.
(68) Bilici, C.; Okay, O. *Macromolecules* **2013**, *46*, 3125.
(69) Wu, L.; Jin, C.; Sun, X. *Biomacromolecules* **2010**, *12*, 235.
(70) Jiang, H. Y.; Kelch, S.; Lendlein, A. *Adv. Mater.* **2006**, *18*, 1471.
(71) Pucci, A.; Bizzarri, R.; Ruggeri, G. *Soft Matter* **2011**, *7*, 3689.
(72) Lendlein, A.; Jiang, H.; Jünger, O.; Langer, R. *Nature* **2005**, *434*, 879.
(73) Kumpfer, J. R.; Rowan, S. J. *J. Am. Chem. Soc.* **2011**, *133*, 12866.
(74) Behl, M.; Zotzmann, J.; Lendlein, A. *Adv. Polym. Sci.* **2010**, *226*, 1.
(75) Lendlein, A.; Kelch, S. *Angew. Chem., Int. Ed.* **2002**, *41*, 2034.
(76) Lendlein, A.; Behl, M.; Hiebl, B.; Wischke, C. *Expert Rev. Med. Devices* **2010**, *7*, 357.
(77) Wischke, C.; Neffe, A. T.; Lendlein, A. *Adv. Polym. Sci.* **2010**, *226*, 177.
(78) Langer, R.; Tirrell, D. A. *Nature* **2004**, *428*, 487.
(79) El Feninat, F.; Laroche, G.; Fiset, M.; Mantovani, D. *Adv. Eng. Mater.* **2002**, *4*, 91.
(80) Yakacki, C. M.; Shandas, R.; Safranski, D.; Ortega, A. M.; Sassaman, K.; Gall, K. *Adv. Funct. Mater.* **2008**, *18*, 2428.
(81) Malda, J.; Visser, J.; Melchels, F. P.; Jungst, T.; Hennink, W. E.; Dhert, W. J. A.; Groll, J.; Hutmacher, D. W. *Adv. Mater.* **2013**, *25*, 5011.
(82) Behl, M.; Razzaq, M. Y.; Lendlein, A. *Adv. Mater.* **2010**, *22*, 3388.